Chapter 4. Submicron and Nanometer Structures Technology and Research

Academic and Research Staff

Professor Henry I. Smith, Richard J. Aucoin, James M. Carter, Robert C. Fleming, Jr., Dr. Mark L. Schattenburg

Visiting Scientists and Research Affiliates

Dr. Khalid Ismail,[1] Yang Zhao,[2] Nubuyoshi Koshida[3]

Graduate Students

Martin Burkhardt, Mike T. Chou, William Chu, Jay N. Damask, Cristopher C. Eugster, Reza A. Ghanbari, Nitin Gupta, Scott D. Hector, Hang Hu, James J. Hugunin, Yao-Ching Ku, Arvind Kumar, Alberto M. Moel, George E. Rittenhouse, Lisa T.-F. Su, Farzam Toudeh-Fallah, Vincent V. Wong, Kenneth Yee, Anthony Yen

Undergraduate Students

Juan Ferrera, Julie C. Lew, Huiying Li, Michael H.Y. Lim, Kristine W. Ma, Chad H. Mikkelson, Euclid E. Moon, Daniel B. Olster, Satyen N. Shah

Technical and Support Staff

Donna R. Martinez, Mark K. Mondol, Jeanne M. Porter, Robert D. Sisson

4.1 Submicron Structures Laboratory

The Submicron Structures Laboratory at MIT develops techniques for fabricating surface structures with feature sizes in the range from nanometers to micrometers and uses these structures in a variety of research projects. These projects, described briefly below, fall into four major categories: (1) development of submicron and nanometer fabrication technology; (2) nanometer and quantum-effect electronics; (3) crystalline films on non-lattice-matching substrates; and (4) periodic structures for x-ray optics, spectroscopy and atomic interferometry.

4.2 X-Ray Nanolithography

Sponsors

Defense Advanced Research Projects Agency
Contract N00019-92-K-0021
Joint Services Electronics Program
Contract DAAL03-92-C-0001
National Science Foundation
Grant ECS 90-16437

Project Staff

Richard J. Aucoin, James M. Carter, William Chu, Robert C. Fleming, Jr., Reza A. Ghanbari, Nitin Gupta, Scott D. Hector, Huiying Li, Alberto M. Moel, Dr. Mark L. Schattenburg, Professor Henry I. Smith, Vincent V. Wong

A large fraction of the applications pursued by the Submicron Structures Laboratory require a reliable lithographic technique capable of producing sub-100 nm features with broad process latitude and high throughput. Ideally, the technique should be simple, low-cost, and enable students to do their own lithography locally. For this reason, we have been developing x-ray nanolithography, exploring its limits, and making its various components (e.g., mask making, resists, electroplating, sources, alignment, etc.) reliable and "user friendly." Because of the critical importance of x-ray mask technology, we discuss this in a separate section (4.3).

---

[1] University of Cairo, Giza, Egypt, and IBM Corporation, Thomas J. Watson Research Center, Yorktown Heights, New York.

[2] Princeton University, Princeton, New Jersey.

[3] Tokyo University of Agriculture and Technology, Tokyo, Japan.

Our sources for x-ray nanolithography are simple, low-cost electron-bombardment targets, typically $Cu_L(\lambda = 1.32$ nm), separated by 1.4 μm-thick SiN_x vacuum windows from the helium-filled exposure chambers. In 1993 we will greatly increase our throughput with a Hampshire Instruments 3500X laser-plasma x-ray source and exposure system. The 3500X will be located in a dedicated room adjacent to the Integrated Circuits Laboratory.

We have developed an apparatus for aligning an x-ray mask to substrates in X, Y and θ and controlling the mask-sample gap. Substrates ranging from 10 cm-diameter Si wafers to 1x1 cm GaAs chips are handled.

In earlier research we showed that for x-ray wavelengths longer than ~ 1 nm, the range of the photoelectron emitted when an x ray is absorbed in resist does not limit resolution. Down to feature sizes ~ 20 nm, diffraction is the only concern. By means of accurate electromagnetic calculations, taking into account the vectorial character of the electromagnetic field and the dielectric properties of the absorber, we have shown that when source spatial coherence is optimized, diffraction does not limit resolution as severely as had been predicted by simple Fresnel diffraction calculations. The results are summarized in figure 1.

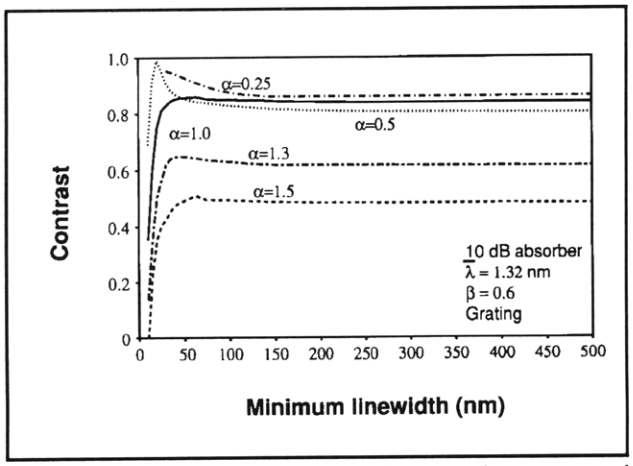

Figure 1. Plot of image contrast for a grating pattern of equal lines and spaces as a function of linewidth, W. The parameter α is related to gap G and wavelength λ via $G = \alpha W^2/\lambda$. β is the ratio of penumbral edge blur to linewidth $\beta = \delta/W$.

For the linewidth range from 70 to 20 nm, mask-substrate gaps must be below 5 μm. This is not a problem in research, but in manufacturing it may be unacceptable. For this reason we are investigating the feasibility of using arrays of zone plates for projection imaging with x rays of either 4.5 nm or ~ 1.2 nm wavelength.

Figure 2 shows the result of two aligned exposures with x-ray nanolithography. This quantum-effect device is an array of quasi-one-dimensional conductors with a crossing tunnel gate.

In the nanolithography range, the final profile obtained in resist depends on both the aerial image and the development characteristics of the resist. We have developed a model and simulation program that enable us to predict resist profiles given the input parameters. We are setting up an apparatus for checking experimentally the simulation.

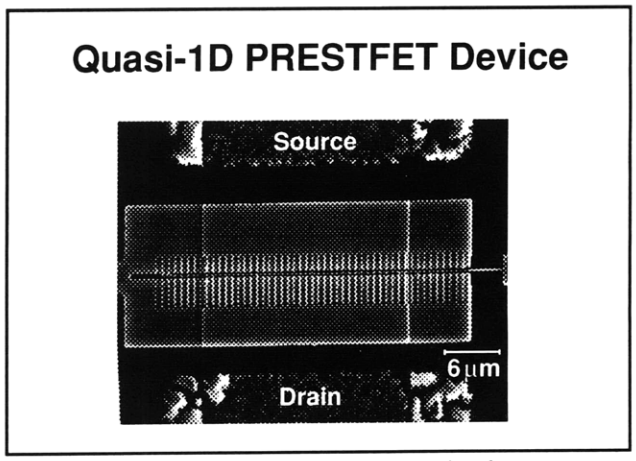

Figure 2. Scanning electron micrograph of a quantum-effect device structure fabricated using two separate, aligned x-ray nanolithography exposures. The master x-ray masks were fabricated at the Naval Research Laboratory (NRL). The device is an array of quantum wires with tunneling barriers in the middle.

4.3 Improved Mask Technology for X-Ray Lithography

Sponsors

Defense Advanced Research Projects Agency
Contract N00019-92-K-0021
National Science Foundation
Grant ECS 90-16437

Project Staff

James M. Carter, William Chu, Juan Ferrera, Robert C. Fleming, Jr., Reza A. Ghanbari, Michael H.Y. Lim, Mark K. Mondol, Dr. Mark L. Schattenburg, Professor Henry I. Smith, Vincent V. Wong

At feature sizes of 100 nm and below, the mask-to-sample gap, G, must be precisely controlled. The mesa mask shown schematically in figure 3 yields mask membranes that are flat to < 250 nm. We are improving this technology with the flip-bonded

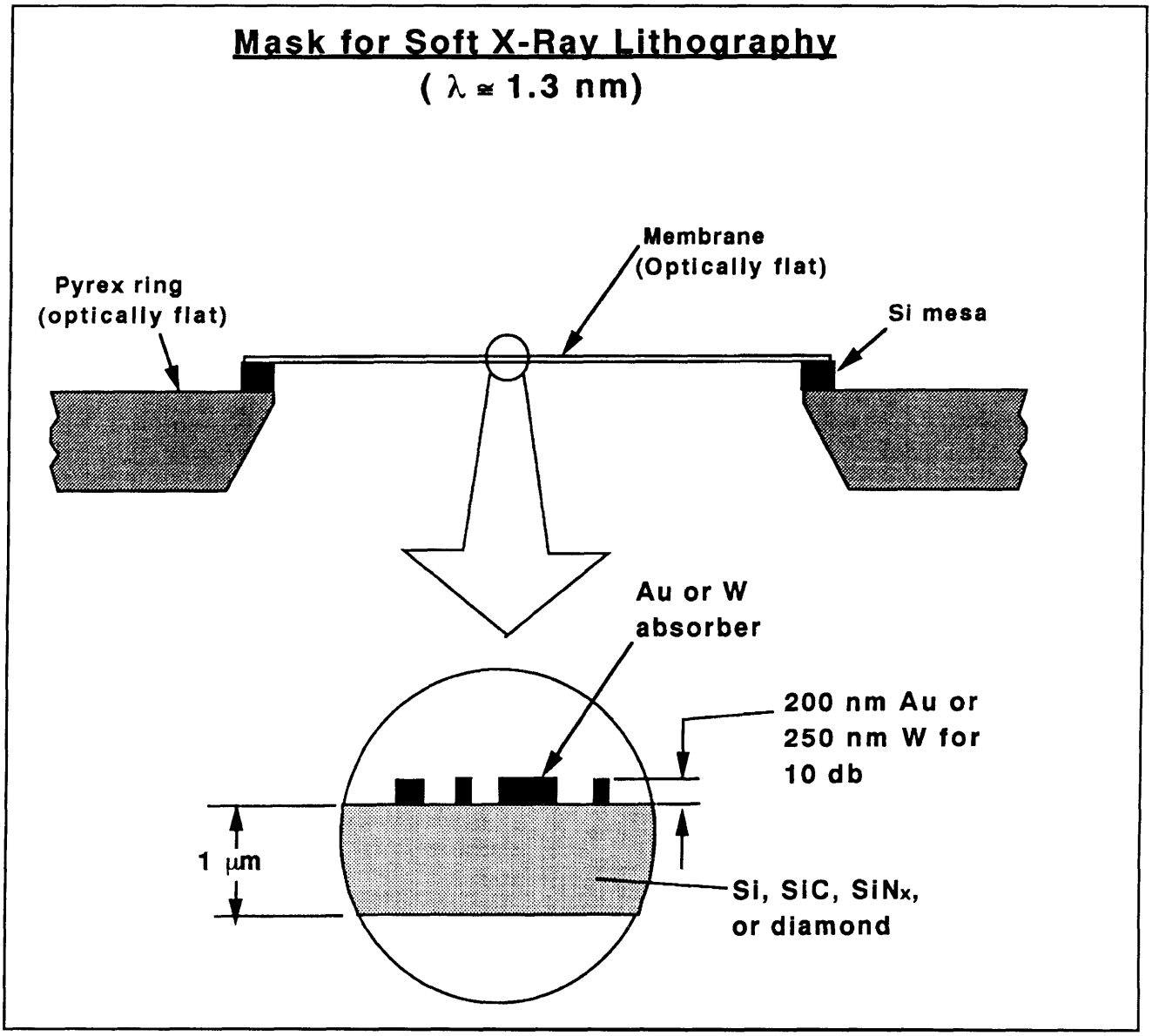

Figure 3. Mesa style mask suitable for x ray lithography at feature sizes from 500 to 20 nm. Membranes are flat to < 250 nm.

scheme shown schematically in figure 4. With this technique, using polysilicon as the anodic bonding agent in place of Ni, we anticipate that x-ray mask blanks can be fabricated entirely with automated integrated circuit (IC) processing equipment.

Our mask technology is based on low-stress, Si-rich silicon nitride, SiN_x. This material is now produced in the IC Laboratory at MIT in a new, dedicated vertical LPCVD reactor. The resulting films are clean and uniform, and x-ray mask membranes made from them are extremely robust. They can be cleaned and processed in conventional stations. Radiation hardness remains a problem at dose levels corresponding to production (i.e., millions of exposures) but for research the material is excellent.

For absorber patterns we use both gold, Au, and tungsten, W. Both can be obtained with near-zero stress (i.e., < 10 MPa) which implies that pattern distortion should be negligible (i.e., < 1 nm). The gold is electroplated onto the membrane after resist exposure and development using a specially designed apparatus. The W is sputter deposited and patterned by reactive-ion etching. We verify the achievement of stress < 10 MPa using a Linnik interferometer, which we have recently equipped with a CCD, a frame grabber, and special purpose software that improves sensitivity.

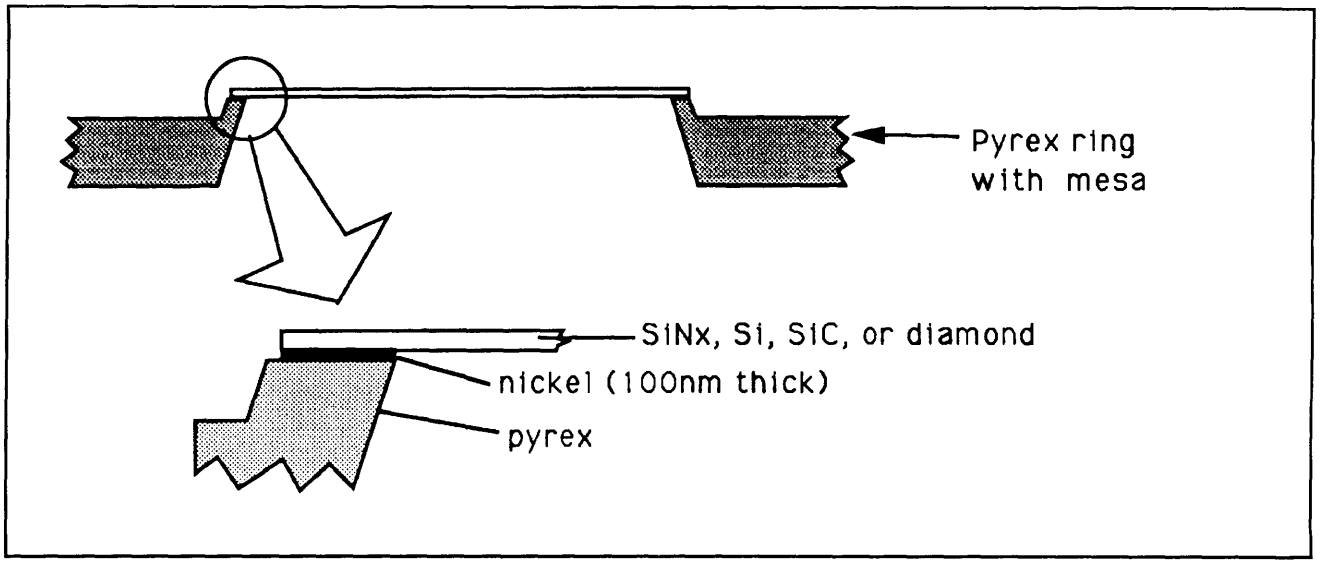

Figure 4. Flip-bonded mask structure in which the mesa rim is formed in the pyrex ring. Membrane flatness is < 100 nm.

In order to check that zero stress, as determined by Linnik interferometry, corresponds to zero in-plane distortion, we have developed a technique of holographic interferometry (HI) shown schematically in figure 5. We have shown a good correlation between Linnik and HI measurements, but we intend to further improve the sensitivity of the in-plane distortion measurements.

Patterning of x-ray masks is done by holographic lithography for periodic structures but, for patterns of arbitrary geometry, is done by e-beam lithography, in collaboration with the Naval Research Laboratory (NRL) and IBM. We use CAD tools at MIT to convert the data into formats compatible with the e-beam exposure systems. Data is shipped to NRL by electronic mail or IBM by express mail along with x ray mask blanks already coated with e-beam resist. After e-beam exposure, the masks are shipped back to MIT by express mail where development and Au electroplating are carried out. This collaboration has already demonstrated that x-ray mask patterning by e-beam can be done remotely, so that university researchers with limited facilities can have access to nanolithography via x ray alone without owning or visiting an e-beam lithography facility.

For the production of x-ray masks with W absorber, a reactive-ion-etching process is required, which puts considerable power into the membrane substrate. Since membranes have very low thermal mass and conductivity, we must heat sink the back side. We are constructing a new reactive-ion-etching system that will provide back-side He cooling. The cooling can be to temperatures as low as -40°C. At such low temperatures the isotropic etching component is suppressed and high resolution directional etching on membranes should be possible.

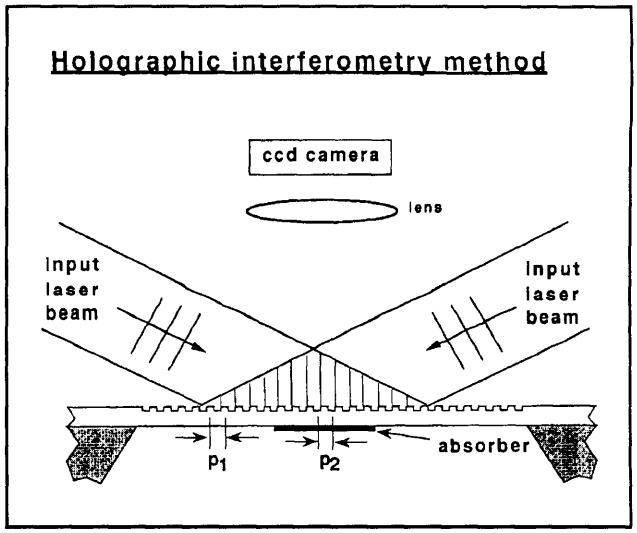

Figure 5. Holographic interferometer for detecting in-plane distortion in x-ray mask membranes.

4.4 Improved Scanning-Electron-Beam Lithography

Sponsors

Joint Services Electronics Program
Contract DAAL03-92-C-0001
U.S. Army Research Office
Grant DAAL03-92-G-0291

Project Staff

Juan Ferrera, Reza A. Ghanbari, Professor Henry I. Smith, Professor Mark L. Schattenburg, Vincent V. Wong

Conventional scanning-electron-beam lithography (SEBL) depends upon laser interferometry to achieve geometric integrity, such as axis orthogonality, accurate length scale, placement accuracy, etc. However, laser interferometry cannot solve all such geometric difficulties, in part because the e-beam location can drift due to thermal expansion, charging, and many other causes. This difficulty with conventional SEBL is particularly troublesome in the fabrication of opto-electronic devices which require spatial-phase fidelity over areas many times larger than a single scan field.

We have proposed a scheme called spatial-phase-locking in order to achieve high fidelity in SEBL. In this scheme, a spatially-coherent grating or grid, created by holographic lithography, is located on the substrate or, in the case of x-ray mask membranes, on a second substrate below. All e-beam writing is then done with reference to this grid using phase locking techniques. Preliminary work has been done in collaboration with IBM Corporation at Yorktown Heights, New York. Whereas in conventional SEBL stitching errors at the boundary of two fields is typically several times 10 nm, we achieved an error below 2 nm. We plan to expand this activity, and, in the long term, we expect to provide an entirely new paradigm for SEBL, which will also translate into lower capital costs.

In order to better predict the optimal SEBL exposure conditions, particularly when writing on x-ray mask membranes, we have implemented a Monte Carlo model for electron scattering and energy loss. A model developed earlier by Hawryluk et al. was modified to include the excitation of secondary electrons. The new model was employed successfully to show that the reduced proximity effect observed by Rhee et al. when SEBL was done over a thin SiO_2 layer on top of tungsten was due to the SiO_2 stopping the energetic secondary electrons from the W.

The new model has also been used to validate the experimentally observed reduction of the deleterious proximity effects due to backscattered electrons when SEBL is done on x-ray mask membranes rather than solid substrates. Figure 6 shows a simulation of resist development following e-beam exposure on (a) a membrane and (b) a solid Si substrate.

4.5 A High-Precision Mask Alignment Scheme

Sponsors

Joint Services Electronics Program
Contract DAAL03-92-C-0001
National Science Foundation
Grant ECS 90-16437

Project Staff

James M. Carter, Robert Frankel,[4] Alberto M. Moel, Professor Henry I. Smith

In order for any lithographic technique to be of general utility, a compatible alignment technique must also be provided. This technique must be capable of superposition precision that is a small fraction of the minimum feature size.

We have demonstrated a novel alignment scheme that builds on the principles of an interferometric scheme we invented several years ago, but overcomes its shortcomings. Alignment marks are simple linear gratings with spatial periods around 1 micron so that the diffraction angle for visible light is around 30 degrees. The spatial periods of the mask and substrate marks differ by a few percent so that beams that are diffracted back onto the optical axis produce a moiré pattern that can be imaged on a CCD. The mask alignment mark also contains a fixed fiducial grating whose spatial period matches that of the moiré pattern. Alignment is defined as that condition wherein the spatial phase of the moiré (which moves as the mask is piezoelectrically displaced relative to the substrate) matches the spatial phase of the fiducial grating.

Using this scheme, a superposition precision with 1 σ equal to 6 nm was achieved, as shown in figure 7. Analysis has shown that the theoretical limit is about 0.6 nm. Clearly, this would be compatible with minimum lithographic features ~ 20 nm, which we consider the practical limit of resist-based lithography.

We plan to work with Hampshire Instruments to develop a commercial version of this alignment scheme and install it in our 3500X x-ray lithography system.

[4] Hampshire Instruments, Inc., Rochester, New York.

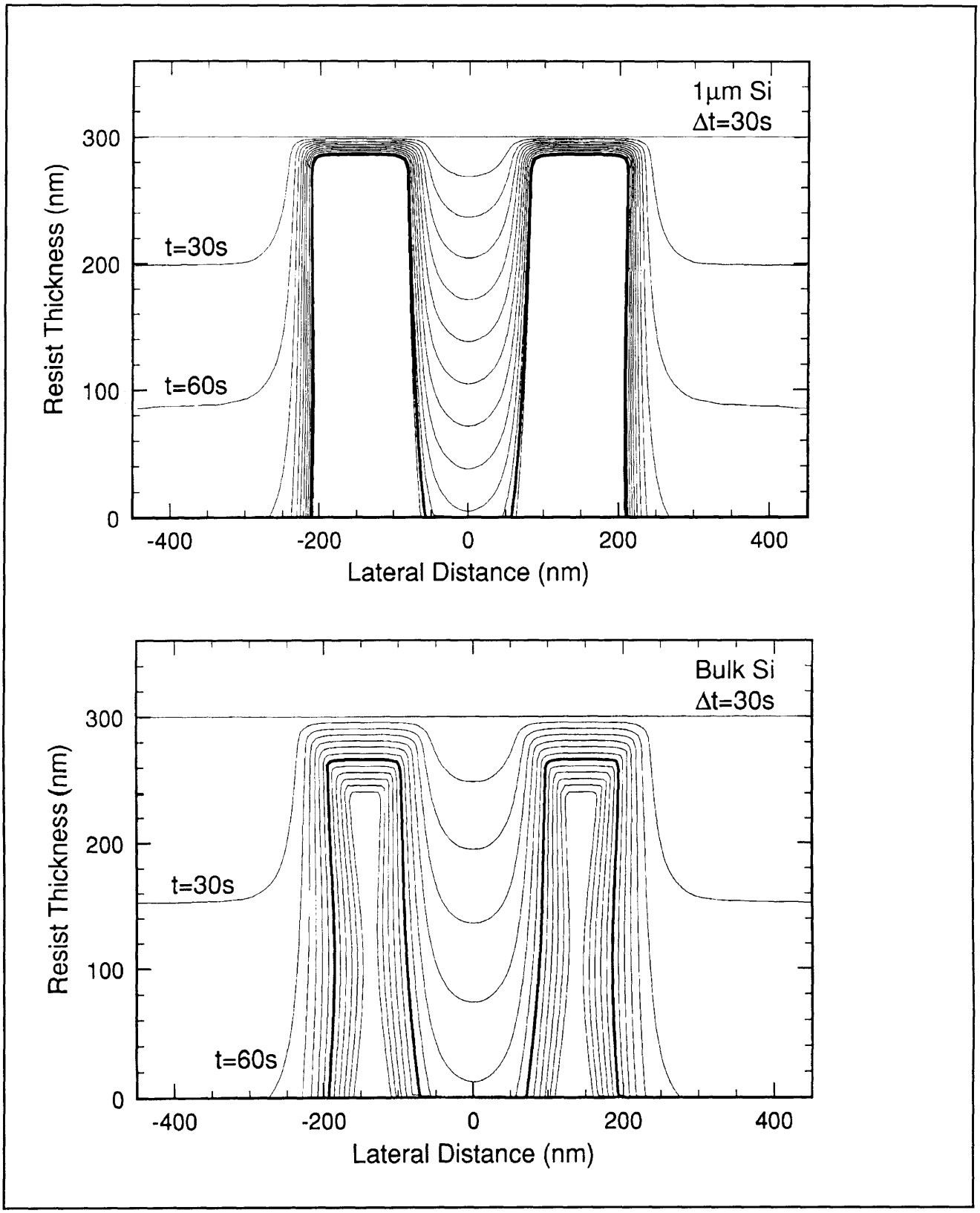

Figure 6. Electron-beam exposure and development simulation for a narrow line running between two large pads exposed at twice the clearing dose. (a) (top) For a 1 μm-thick Si membrane substrate, (b) (bottom) For a solid substrate. Successive contours represent 30 sec of additional development. Note the reduction of proximity effects for exposure on a membrane substrate.

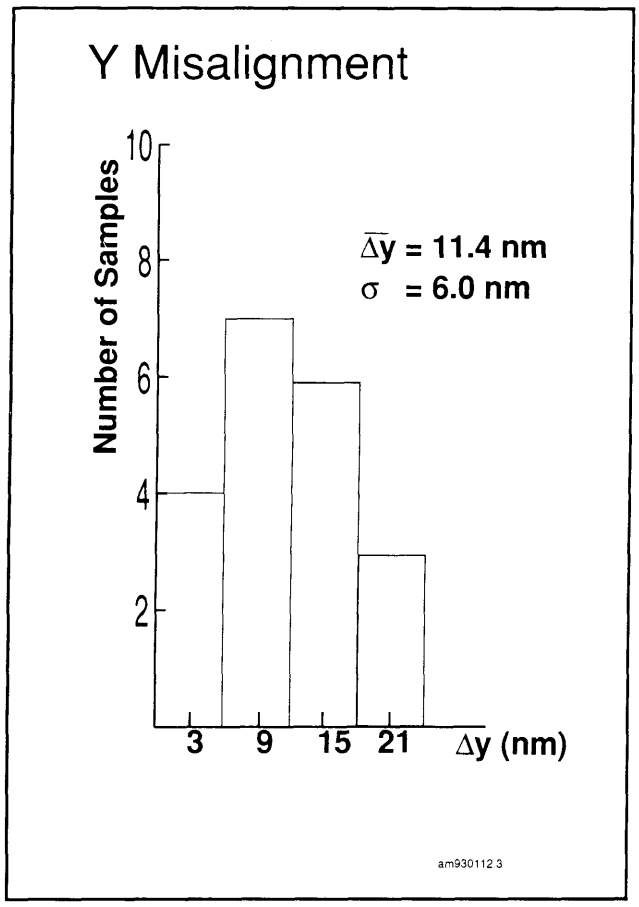

Figure 7. Histogram of 20 successive aligned x-ray exposures, showing σ = 6 nm. Offset of peak is not significant. A moiré method was used to measure misalignment.

4.6 Achromatic Holographic Lithography

Sponsor

Joint Services Electronics Program
Contract DAAL03-92-C-0001

Project Staff

Scott D. Hector, Satyen N. Shah, Professor Henry I. Smith

Holographic schemes are preferred for the fabrication of periodic and quasi-periodic patterns that must be spatially coherent over large areas and free of phase steps. For spatial periods below 200 nm light sources with wavelengths below 200 nm must be used. All such sources have limited temporal coherence, and thus one is forced to employ achromatic schemes such as shown in figure 8. Using this apparatus, we have achieved gratings of 100 nm period (i.e., 50 nm lines and spaces). In order to make the apparatus more reliable the depth-of-focus has to be increased, which implies an improvement of the source spatial coherence. To this end, we have introduced a collimating lens and a slit scanning system. In order to enhance yield and area, it will be necessary to find the substrate location that provides maximum image contrast. Therefore, we have set up a white-light interferometer that utilizes optical paths through the quartz plates that closely approximate the paths of the exposing beams. A photodetector and lock-in amplifier will be used to find the optimum sample position.

Once the system is fully reliable, we plan to take the technique one step further to 50 nm periods (25 nm lines and spaces) using a 13 nm undulator as the light source.

4.7 Fabrication of T-gate Devices using X-ray Lithography

Sponsor

Defense Advanced Research Projects Agency
Contract N00019-92-K-0021

Project Staff

James M. Carter, Nitin Gupta, Professor Henry I. Smith

High-speed MODFET devices require very short gate lengths while preserving low resistance. Large gate widths are required for high current drive. To meet these conflicting demands, researchers have developed so-called "T-gate" and "gamma-gate" processes in which the base of the gate is very short (~ 100 nm) while the upper part is large and overlaps the short base, like a mushroom or the letters T or gamma. Such structures are readily achieved using direct-write electron-beam lithography. However, this technology is expensive, slow, and probably incompatible with mass production.

For these reasons, we are developing an x-ray lithography-based approach to making Tee and gamma gate devices. Several schemes are being pursued. The most straightforward involves a tri-layer resist. The first layer is an x-ray sensitive resist (e.g., PMMA or a chemically amplified novolak), the second is a barrier layer (e.g., photosensitive polyimide) between the x-ray resist and the upper layer, which is photoresist. The upper layer and the polyimide are exposed with UV light. This tri-level process provides maximum flexibility and a large process window, but requires two separate alignments and exposures. On the other

Achromatic Holographic Lithography

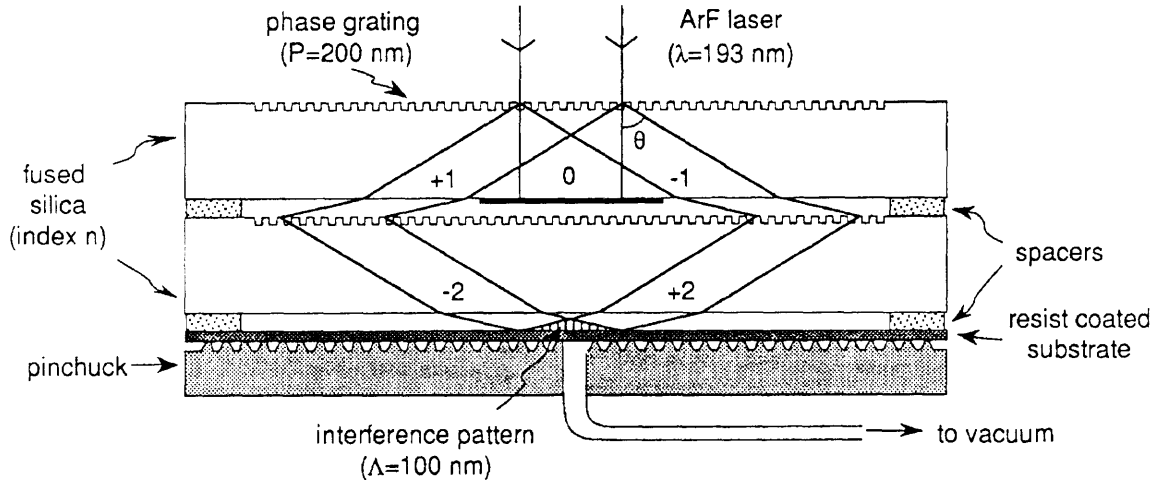

$$\sin\theta = \lambda/(nP),$$

$$\Lambda = \lambda/(2n \sin\theta)$$

$$= P/2$$

Figure 8. Achromatic holographic lithography configuration for generating 100-nm-period gratings.

hand, the photolithography does not have to be aligned as precisely as the x-ray exposure. Other approaches will also be investigated in which, for example, three different x-ray resist sensitivities are employed and only one alignment and exposure is needed.

4.8 Tenth-micron MOSFET Device Technology

Sponsors

IBM Corporation
Joint Services Electronics Program
Contract DAAL03-92-C-0001

Project Staff

Professor Dimitri A. Antoniadis, Professor James E. Chung, Dr. Hao Fang, Hang Hu, Professor Henry I. Smith

We have continued using x-ray lithography to fabricate both N- and P- channel MOSFET devices with effective channel lengths down to 80 nm. The emphasis is on investigating hot-carrier quasi-ballistic transport processes.

A new generation of x-ray masks capable of defining sub-0.1 μm polysilicon gates and compatible with conventional MOSFET device and circuit processing were successfully developed and tested. A portion of a ring oscillator circuit, patterned in Au on an x-ray mask, is shown in figure 9. A chemically amplified resist (PF-514) is used for the 0.1 μm gate definition, as shown in figure 10.

Self-aligned P-channel MOSFET devices were fabricated on N-type, 20 Ω-cm (100) silicon substrates. In order to maximize channel hole mobility and to control deep punchthrough down to L_{eff} of 0.1 μm, super-steep-retrograde (SSR) channel doping was used. It consists of phosphorus ion implantation with energy of 180 KeV and dose of 5.0×10^{12} cm^{-3}, and arsenic ion implantation with energy ranging from 70 KeV to 94 KeV and dose ranging from 4.0×10^{12} cm^{-3} to 1.0×10^{13} cm^{-3}. The 5.2 nm thick gate oxide was thermally grown at 800° C. In order to form the P^+-N source-drain junctions, germanium was first implanted to amorphize the source-drain area and a BF_2 implant with energy of 10 KeV and dose of 4.0×10^{14} cm^{-3} was carried out to form the shallow P - N junction extensions. A 10 nm thick oxide spacer was then formed. A second BF_2 implant with energy of 20 KeV and dose of 5.0×10^{15} cm^{-3} formed the P^+ - N junctions in the area defined by the previously formed oxide spacer. The P^+ - N junction annealing consisted of a 600°C, 30 min furnace diffusion followed by 10 sec RTA at 1000°C. Self-aligned cobalt silicide with thickness of about 40 nm was formed to reduce the sheet resistance of the source-drain junctions. Typical values of total source and drain resistance were about 850 Ωμm. Finally, CVD oxide contact cuts and aluminum contacts were formed to the gates and the source-drain regions.

Two SSR channel doping profiles calculated by SUPREM-III are shown in figure 11. Two sets of P-MOSFETs with L_{eff} ranging from 0.1 μm to 10 μm obtained with these two SSR doping profiles all exhibit excellent punchthrough characteristics. The I - V characteristics of 0.1 μm P-MOSFET devices at 300 K and 77 K is shown in figure 12. The peak hole mobility at low longitudinal E - field was 92 $cm^2/V\text{-}s$. The room temperature threshold voltage was -0.4 V. This shows that a good compromise between reducing short channel effects and maintaining practical device integrity is reached for 0.1 μm scale P-channel MOSFET devices with SSR channel doping profiles.

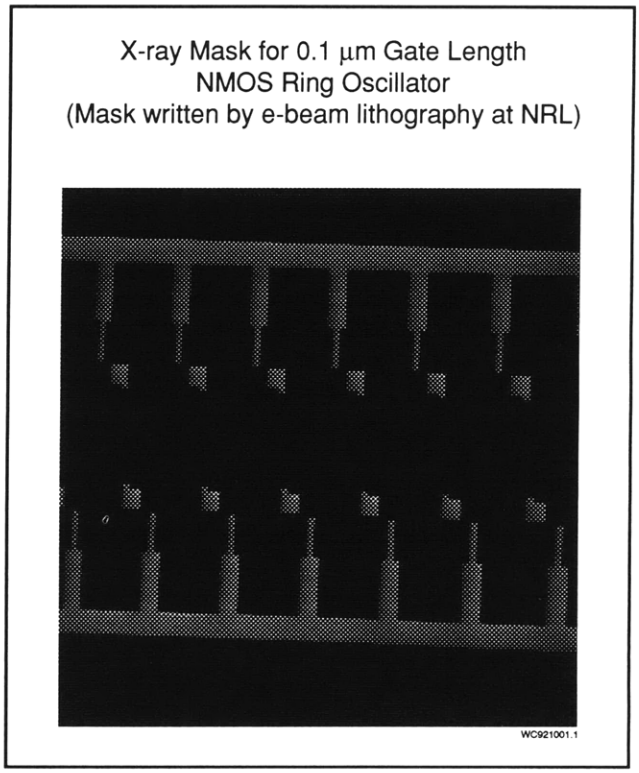

Figure 9. X-ray mask of a 0.1 μm gate-length NMOS ring oscillator (x-ray mask written by e-beam lithography at the Naval Research Laboratory).

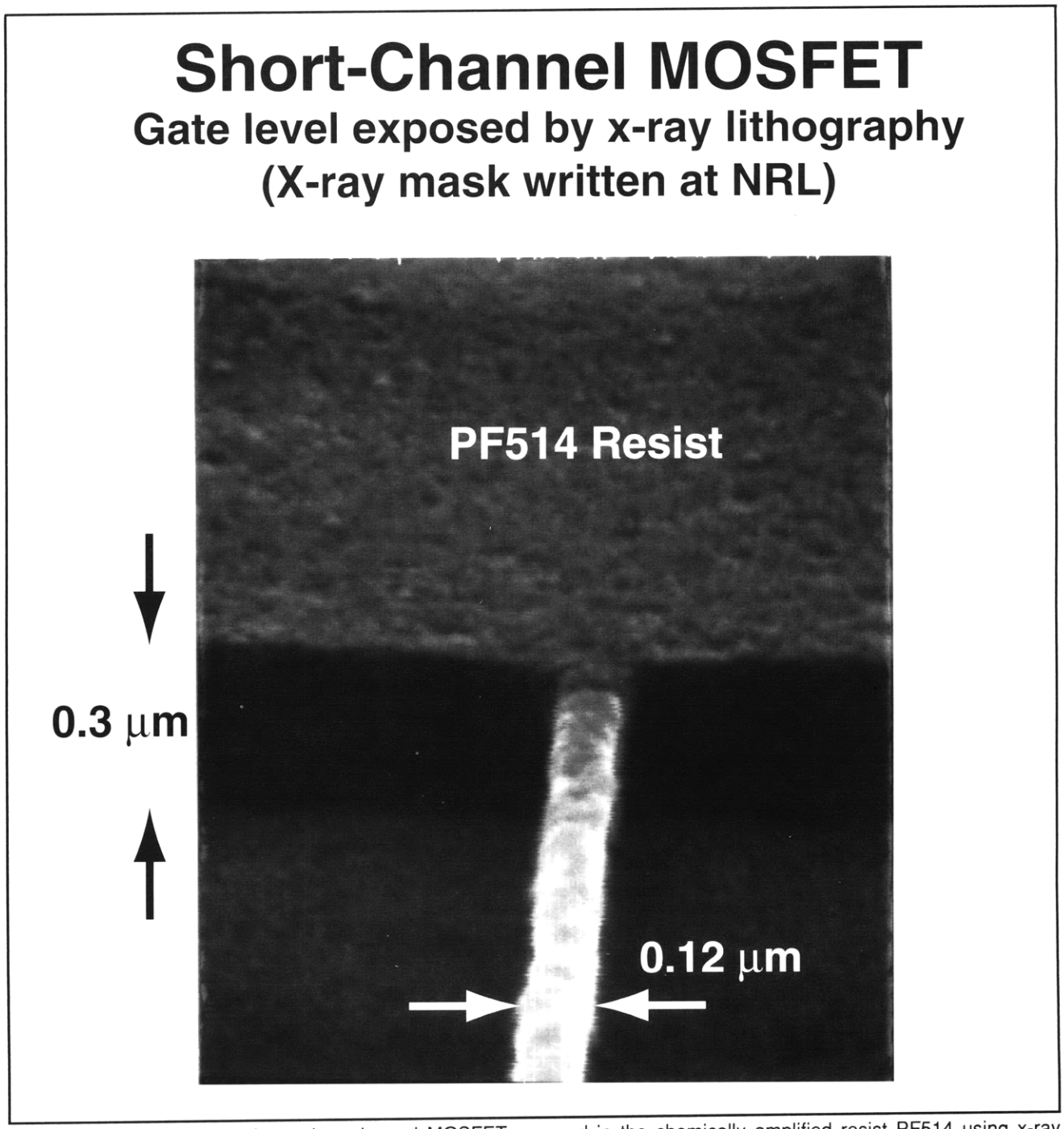

Figure 10. Resist pattern for a short-channel MOSFET exposed in the chemically amplified resist PF514 using x-ray lithography at $\lambda = 1.32$ nm.

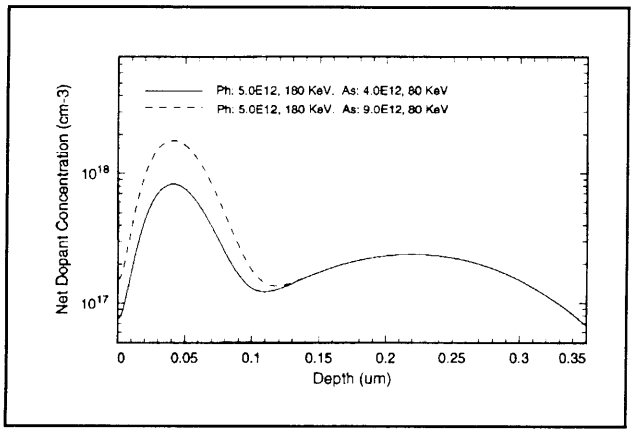

Figure 11. Dopant concentration as a function of depth as calculated by Supreme III.

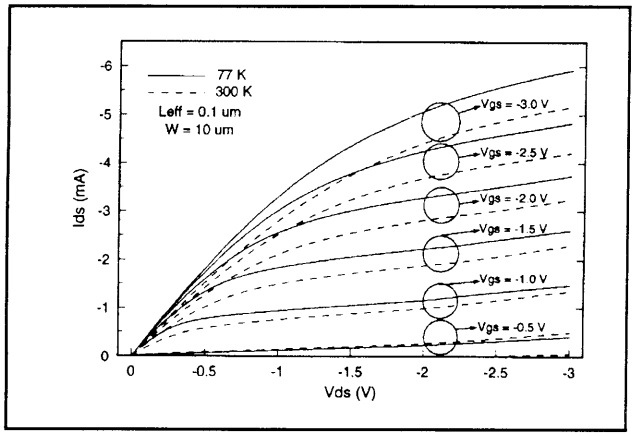

Figure 12. I-V characteristics of 0.1 μm PMOSFET devices at 77 K and 300 K.

4.9 Studies of Coulomb Charging Effects in Semiconductor Nanostructures

Sponsor

U.S. Air Force - Office of Scientific Research
Grant F49620-92-J-0064

Project Staff

Professor Dimitri A. Antoniadis, William Chu, Cristopher C. Eugster, Arvind Kumar, Professor Terry P. Orlando, Michael Rooks[5]

Many novel effects have been observed in the transport properties of ultrasmall "quantum-effect" transistors whose feature size is comparable to the electron Fermi wavelength (about 50 nm in a typical inversion layer). In addition to the prominent role played by these effects in solid-state physics, they have great potential in the technology of the electronics revolution.

In a "quantum dot" device, an electron gas is confined electrostatically in all three spatial dimensions, forming a small "puddle" of electrons bounded on all sides by a potential wall. This small electron "puddle" resembles an atom in that there can only be an integer number of electrons, and these electrons can occupy only certain discrete energy levels.

Recent low-temperature experiments on transport through a narrow electron channel interrupted by two tunnel barriers—forming an isolated electron "quantum dot"—have found that the conductance through the dot consists of a series of sharp maxima which occur periodically as the voltage on the transistor gate is varied. This remarkable conductance modulation arises from the condition of charge quantization inside the dot. Each successive conductance maximum corresponds to the discrete addition of a single electron to the dot. Between successive conductance peaks, the resistance increases by several orders of magnitude because there is a large energy cost for an electron in the contact to enter the dot. This energy cost can be removed by changing the gate voltage, resulting in the observed periodic dependence of the conductance on gate voltage.

This conductance modulation through an electron puddle has been studied extensively and is now well understood. We propose to study a device structure with two electron puddles which can interact with each other through a thin tunnel barrier. In addition to exploring new physics, we are motivated by the consideration that such a coupled system would represent the first step toward an architecture in which two elements could interact with each other without an interconnect. Figure 13 shows a scanning electron micrograph of the gate geometry of our device structure, fabricated by electron beam lithography at the National Nanofabrication Facility. A negative voltage applied to the gates depletes the high-mobility two-dimensional electron gas (2DEG) underneath, which is formed at the GaAs/AlGaAs interface, leaving behind two small electron puddles. Four ohmic contacts at the corners allow access to the 2DEG; both series and parallel combinations of the dots can be realized depending on the bias voltages.

[5] Cornell University, Ithaca, New York.

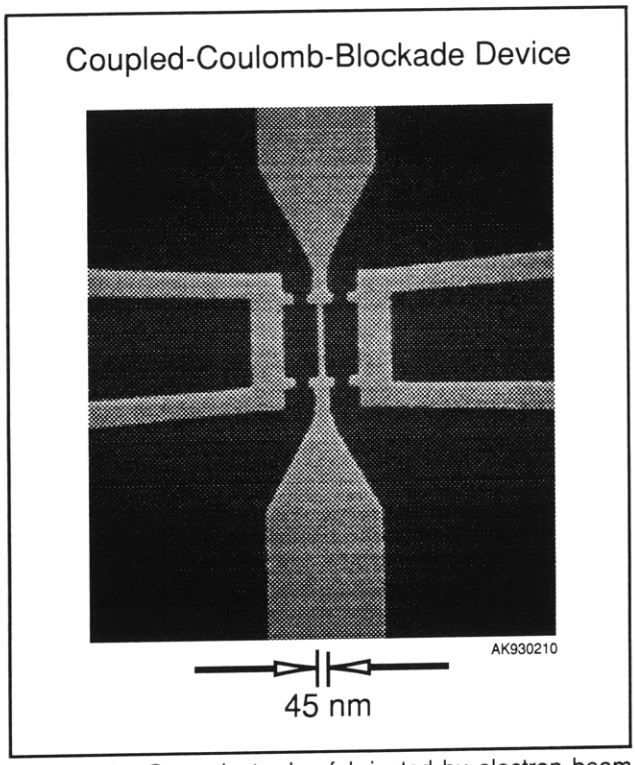

Figure 13. Gate electrodes fabricated by electron beam lithography and liftoff over a GaAs/AlGaAs heterostructure. A negative voltage on the gate electrodes depletes the 2DEG underneath, leaving behind two electron islands. Ohmic contacts at the four corners allow access to the 2DEG.

We are also working on studying Coulomb charging effects in devices fabricated by x-ray lithography. Figure 14 shows a scanning electron micrograph of an x-ray mask which will be used for patterning the gate geometry of a device with a single electron puddle. The corresponding device will offer independent control of the potential barriers confining the dot and the number of electrons occupying the dot. This independent control has been found in previous experiments to improve the yield of devices showing Coulomb blockade effects.

4.10 Study of Quasi-One-Dimensional Wires in GaAs/AlGaAs Modulation Doped Field-Effect Transistors

Sponsor

U.S. Air Force - Office of Scientific Research
Grant F49620-92-J-0064

Project Staff

Professor Dimitri A. Antoniadis, Martin Burkhardt, William Chu, Professor Jesús A. del Alamo, Reza

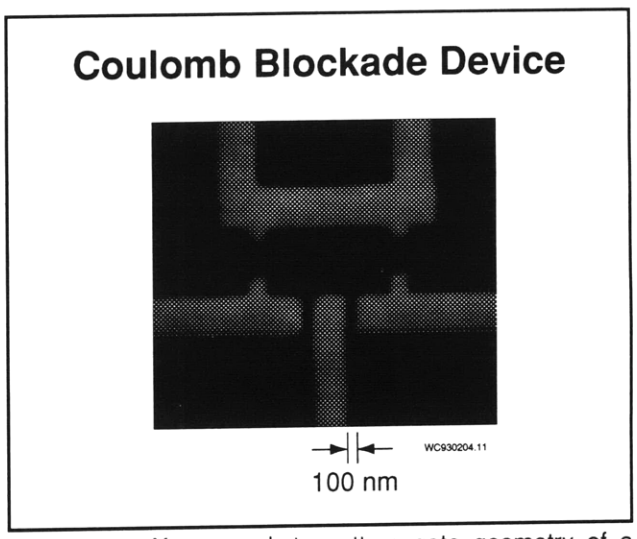

Figure 14. X-ray mask to pattern gate geometry of a quantum dot device with a single electron puddle. Note that the potential barrier at each constriction and the number of electrons in the dot can be controlled independently.

A. Ghanbari, Professor Terry P. Orlando, Professor Henry I. Smith

We have successfully fabricated quasi-one-dimensional (Q1D) wires using x-ray lithography and precise chemical etching. These devices were fabricated on a high quality GaAs/AlGaAs modulation-doped substrate. By first patterning the wires using x-ray lithography, then chemically etching the GaAs, the region under the etched areas become depleted of electrons, leaving behind many parallel quasi-one-dimensional wires. A schematic cross-section of this device is shown in figure 15.

Because the operation of this device depends critically on the shape of the confinement potential, control of the etch depth is crucial. Dry etching techniques have sufficient repeatability for this application, but they cause an unacceptable amount of damage to the substrate. Chemical etching minimizes damage but has a very unpredictable etch rate.

To overcome these difficulties, a high precision interferometric technique was developed that is capable of resolving depth changes of less than 1 nm. By capturing the image formed in a Linnik interferometer and using Fourier analysis techniques, we can monitor the etch depth with a precision < 1 nm, permitting the reliable fabrication of these devices.

When the Q1D devices are measured at cryogenic temperatures, the quantum confinement clearly manifests itself as a nonlinear conductance, as shown in figure 16. Each nonlinear bump in the

transconductance (shown in the insert in figure 16) corresponds to the Fermi level passing through different subbands of the Q1D confining potential. A schematic of the confinement potential, as seen by electrons traveling down the wire, is shown in figure 17.

Work is currently underway to harness these Q1D wires in a new type of planar resonant-tunneling device with Q1D emitter and collector (Q1D-PRESTFET) that has been predicted to show very strong non-linearities in conductance.

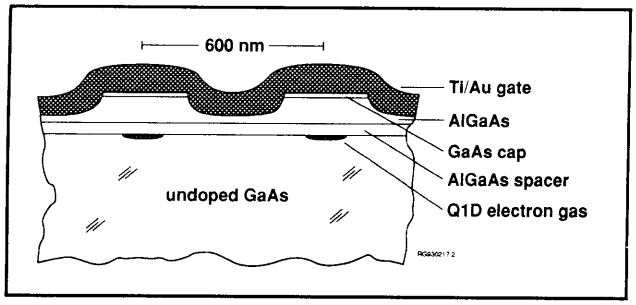

Figure 15. Schematic cross-section of completed quasi-one-dimensional device.

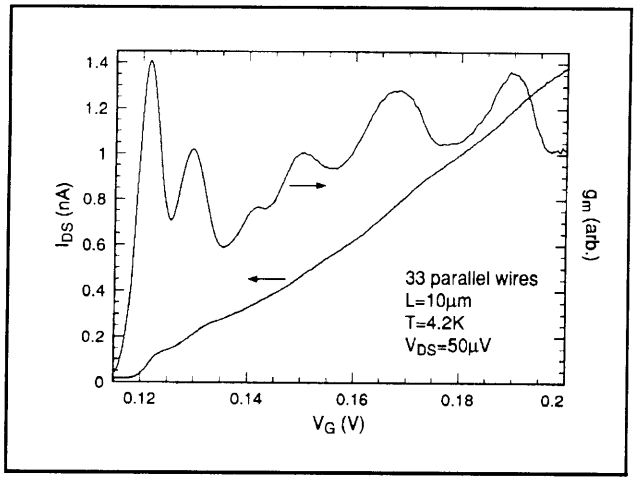

Figure 16. Measured conductance and transconductance for a multiple-parallel quasi-one-dimensional device.

4.11 Planar-Resonant-Tunneling Field-Effect Transistors (PRESTFET)

Sponsor

U.S. Air Force - Office of Scientific Research
Grant F49620-92-J-0064

Project Staff

Professor Dimitri A. Antoniadis, Mike T. Chou, William Chu, Martin Burkhardt, Professor Henry I. Smith

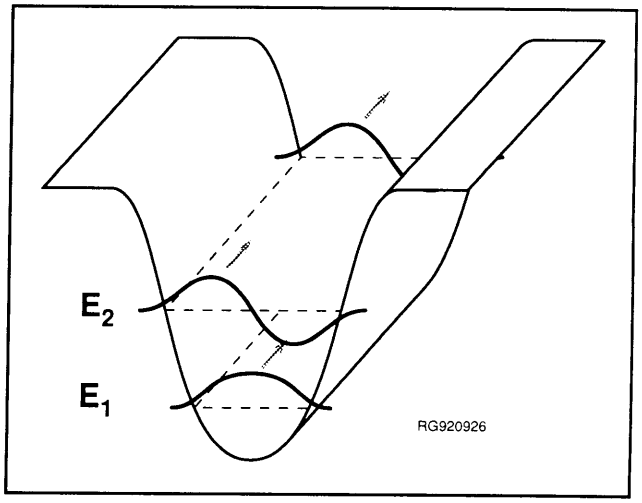

Figure 17. Schematic of potential seen by electrons traveling along a Q1D wire (arrows indicate direction of current flow).

Planar-resonant-tunneling field-effect transistors were built on modulation doped GaAs/AlGaAs substrates using x-ray lithography, making it possible to achieve good step coverage onto a 120 nm high mesa, as shown in figure 18. This device, with 200 nm gate pitch, showed good transistor characteristics but coherent resonant tunneling between source and drain was not observed. Efforts are underway to shrink the gate pitch to 150 and 100 nm. We expect to see resonant tunneling in these devices at liquid Helium temperature.

We are also investigating the feasibility of PRESTFETs in Si. Top and sideviews of the device are shown in figure 19. This device has a two-level gate structure. A very thin, high-quality layer of silicon dioxide (~ 10 nm) is grown on a p-type silicon substrate. Then, two parallel tunneling electrodes (lower level gates) will be patterned in polysilicon using x-ray lithography and liftoff. A thin layer (~ 10 nm) of insulating silicon nitride will be deposited over this structure. Finally, a large metal gate (the upper level gate) will be deposited over the silicon nitride. A two-dimensional electron gas (2-DEG) will be formed at the Si/SiO_2 interface by applying a positive bias to the upper gate. Tunnel barriers in the 2-DEG will be created directly underneath the lower gates by applying appropriate bias voltages.

This silicon PRESTFET offers the exciting possibility of potential modulations over extremely small distances (on the order of 10 nm). For the equivalent GaAs device, the distance between the gate electrodes and the 2-DEG is limited to the minimum thickness of the n-doped AlGaAs layer that is required to achieve a certain electron concentration at the 2-DEG (i.e., about 50 nm). The main disad-

vantage of the silicon system is its low mobility compared to GaAs. But, if we optimize the Si/SiO_2 interface quality by avoiding contamination and controlling the damage caused by processing steps, it is possible to obtain an interface defect/impurity concentration as low as $1 \times 10^{10}\ cm^{-2}$. This implies an average spacing between defects of about 100 nm. Since our goal for the silicon PRESTFET is to fabricate a 50 nm-wide quantum well sandwiched between two 50 nm-wide barriers, carrier mobility, and hence scattering, should not be a fundamental limitation. We expect to observe quantum transport effects at 4.2 K.

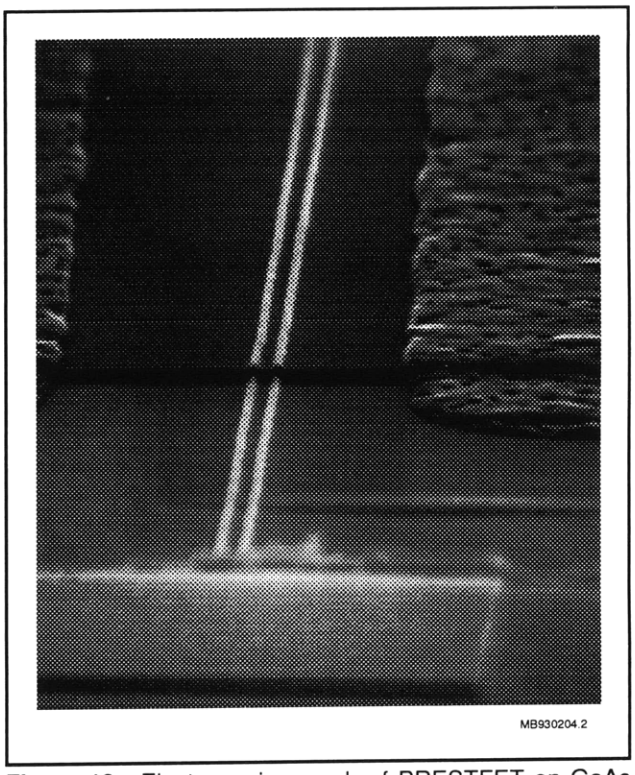

Figure 18. Electron micrograph of PRESTFET on GaAs fabricated using x-ray lithography, which enables good step coverage up onto the 120 nm-high mesa.

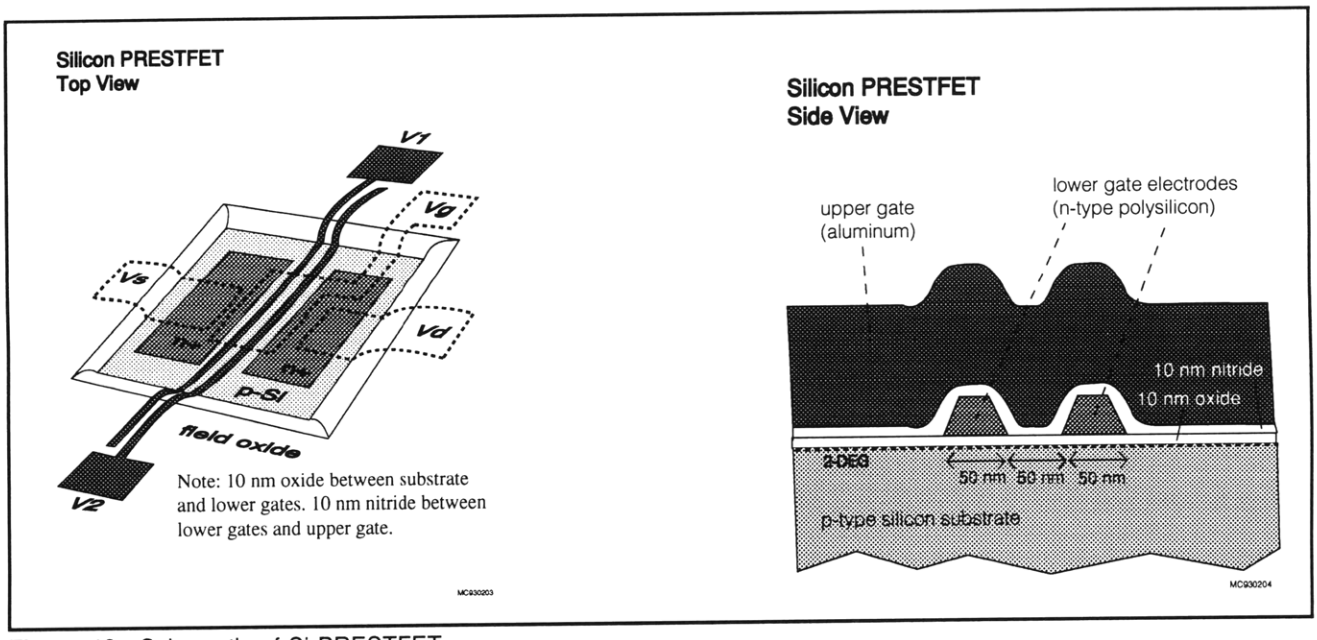

Figure 19. Schematic of Si PRESTFET.

4.12 Dual Electron Waveguide Device Fabricated using X-ray Lithography

Sponsor

National Science Foundation
Grant DMR 87-19217
Grant DMR 90-22933

Project Staff

Professor Jesús A. del Alamo, William Chu, Cristopher C. Eugster, Professor Henry I. Smith.

We have recently fabricated a dual-electron-waveguide device, shown in figure 20, using x-ray nanolithography. An electron waveguide is essentially a one-dimensional channel which electrons can travel through without scattering. In our device, two such channels are electrostatically formed in close proximity of each other by depleting those electrons in an AlGaAs/GaAs modulation-doped heterostructure which reside underneath the three gates shown in figure 20. The x-ray mask used in the fabrication process was patterned using 50 keV e-beam lithography at the Naval Research Laboratory. We use x-ray lithography to replicate this mask to change its polarity. Then we align the new mask to the AlGaAs/GaAs sample and expose it using contact x-ray nanolithography.

In an electron waveguide, similar to an optical waveguide, discrete transverse modes arise due to the lateral confinement. The conductance of each waveguide mode is equal to a fundamental constant 2 e^2/h. This results from the cancellation of the energy dependence in the product of the 1D density of states and the electron velocity. In recent experiments on x-ray fabricated dual electron waveguide devices, quantized conductance for each waveguide was observed as the number of occupied modes was electrostatically varied.

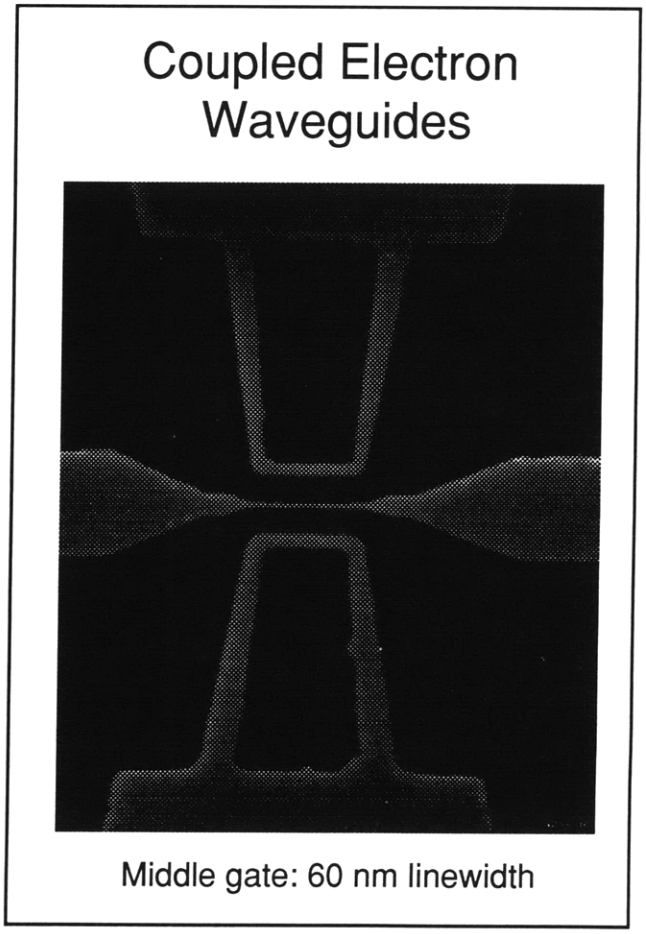

Figure 20. Electron micrograph of dual-electron-waveguide device fabricated using x-ray nanolithography.

Project Staff

Professor Dimitri A. Antoniadis, Martin Burkhardt, Reza A. Ghanbari, Professor Terry P. Orlando, Professor Henry I. Smith, Professor M. Shayegan,[6] Song Sang-hun,[6] Professor Daniel Tsui,[6] Kenneth Yee, Yang Zhao

In collaboration with researchers at Princeton University, we have used x-ray lithography to fabricate devices for magneto-optic measurements of a two-dimensional electron gas (2DEG). Metal grids with spatial periods of 300-600 nm in both orthogonal directions and covering several square millimeters were placed on the surface of a modulation-doped AlGaAs substrate. The grids were used to periodically modulate far-infrared radiation (FIR) incident on the 2 DEG. Due to the close proximity of the grids to the heterointerface (~ 50 nm), it was possible to access an electron-electron interaction effect by the FIR radiation at the wave vectors of

4.13 Far-Infrared Spectroscopy of Arrays of Quantum Dots and Wires

Sponsors

Joint Services Electronics Program
Contract DAAL03-92-C-0001
U.S. Air Force - Office of Scientific Research
Grant F49620-92-J-0064

[6] Princeton University, Princeton, New Jersey.

the metal grid. These spectra were observed as a function of magnetic field. Results were in agreement with theoretical models.

Using similar lithographic techniques, metal gratings with spatial periods of 300-600 nm were placed on modulation-doped substrates (figure 21a), and a gate electrode was attached to the grating. Depending on the applied gate voltage, the potential seen by the electrons at the 2DEG can be varied from uniform (in which case the electrons behave as a normal 2 DEG) to weakly-coupled quantum wires (figure 21b), or to isolated quantum wires (figure 21c). These quantum-wire structures were measured using FIR cyclotron resonance. Mode softening due to quantum-mechanical coupling between wires was observed. The results were in agreement with theoretical models of coupled-quantum wires.

Arrays of etched quantum dots, quantum wires, and quantum anti-dots have also been fabricated, with typical spatial periods of 300-600 nm. The electronic subbands of these structures were also examined using FIR cyclotron resonance. Currently, we are continuing our study using extremely high-quality samples prepared by Professor Shayegan's group at Princeton.

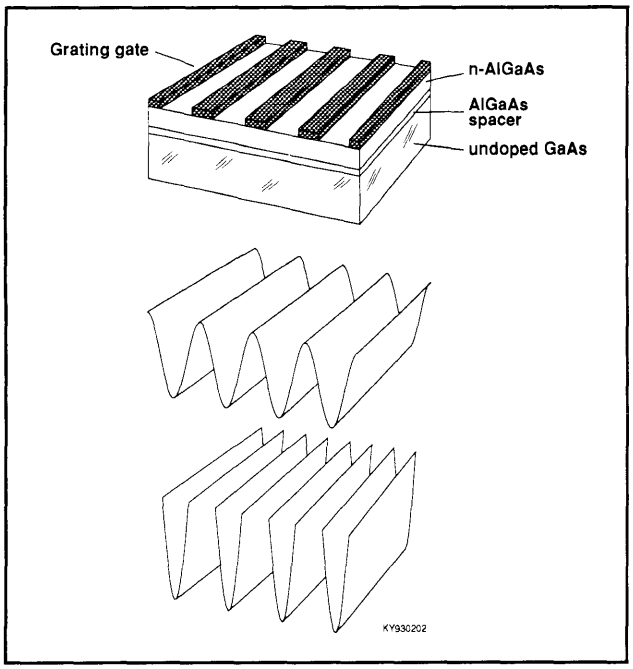

Figure 21. (a) Metal grating gate on a modulation-doped AlGaAs/GaAs substrate; (b) depiction of potential seen by electrons at the AlGaAs/GaAs interface for weakly coupled quantum wires; (c) potential for the case of isolated quantum wires.

4.14 Ridge-Grating Distributed-Feedback Lasers Fabricated by X-Ray Lithography

Sponsor

U.S. Army Research Office
Grant DAAL03-92-G-0291

Project Staff

James M. Carter, Woo-Young Choi, Juan Ferrera, Professor Clifton G. Fonstad, Jr., Professor Henry I. Smith, Vincent V. Wong

Distributed-feedback lasers (DFB) are essential components in optical communications systems because they operate in a single-longitudinal-mode and are easily integrable with electronic drive circuitry. In the fabrication of a typical DFB laser, an epitaxial regrowth step is carried out on top of the grating, which can be yield-limiting. In particular, because of etch back, the coupling constant after epi-growth can be difficult to predict. In the following paragraphs we describe a novel DFB laser that eliminates the need for regrowth and maximizes the utility of ridge-waveguide devices which are much simpler to fabricate.

To realize such a device structure, we have developed a fabrication process that utilizes x-ray lithography for the grating fabrication because it offers good process latitude, high throughput, long-range spatial-phase fidelity in the gratings, and large depth-of-focus, which is essential for sidewall patterning. A schematic of the ridge-grating DFB laser is shown in figure 22. After the epitaxial growth of a complete InGaAlAs graded-index, separate-confinement, multi-quantum-well-layer diode structure by molecular-beam epitaxy on an InP substrate, a 3-4 μm-wide ridge waveguide is formed by wet-etching. The wet-etching conditions are carefully controlled so that the desired side-wall profile is obtained. A first-order grating with a period of 230 nm for the target lasing wavelength of 1.55 μm is then patterned in resist using x-ray lithography. The Cu_L-line (λ = 1.32 nm) of an electron-bombardment source is used in conjunction with SiN_x mask technology. The x-ray mask is patterned using holographic lithography, which guarantees excellent uniformity and long-range spatial-phase coherence in the grating, followed by gold electroplating. Dry-etching is used to transfer the grating into both sides of the ridge waveguide. With this ridge-grating, the optical feedback occurs via the interaction of the lateral fields with the index modulation introduced by the grating. Holographic lithography could not be used directly for the grating exposure because of troublesome coherent reflec-

tions from the ridge topography. For advanced optical communication systems (e.g., those implementing wavelength-division multiplexing), quarter-wave-shifted DFB lasers, hundreds of microns in length, are necessary. This will require e-beam lithography that is free of distortion and stitching errors for the x-ray mask making. As described in section 4.4, we are pursuing a technique based on a global-fiducial grid scheme which can potentially solve both of these problems. Once developed, this technique will be incorporated into the e-beam lithography process to define the appropriate DFB laser grating patterns onto a SiN_x x-ray mask.

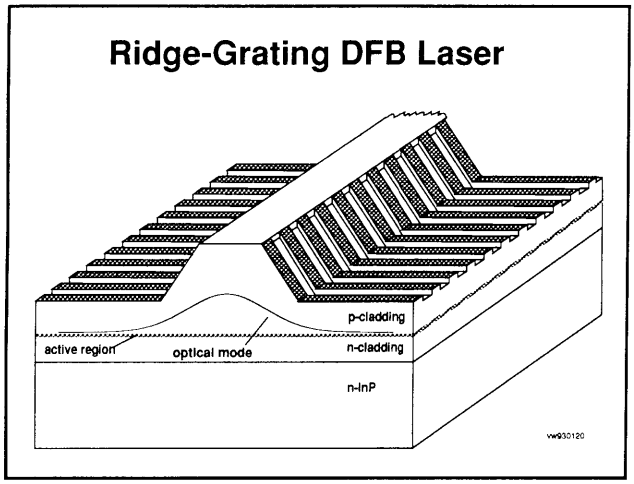

Figure 22. Schematic of ridge-grating DFB laser.

4.15 Channel-Dropping Filters Fabricated by X-Ray Lithography

Sponsor

U.S. Army Research Office
Grant DAAL0-92-G-0291

Project Staff

Jay N. Damask, Professor Hermann A. Haus, Professor Leslie A. Kolodziejski, Professor Henry I. Smith, Vincent V. Wong

Channel-dropping filters are novel optoelectronic devices that can extract a signal of a particular wavelength from an optical bus carrying multiple-signals. The extraction is achieved through the interaction of three coupled waveguides. A schematic of a channel-dropping filter (CDF) is shown in figure 23. The middle waveguide, which carries several signals, is side-coupled to two quarter-wave-shifted grating resonators. These grating resonators are resonant at frequency f_2 and serve to extract this particular frequency component from the center waveguide.

For our initial demonstration of the CDF concept, we are working with a SiO_2/Si_3N_4-layered system. For this materials system, grating periods tailored for a center optical wavelength of 1.55 μm will be approximately 515 nm. X-ray lithography will be used to transfer the grating pattern onto ridge waveguides fabricated by wet-chemical etching. The patterning of the necessary x-ray mask poses a significant challenge to existing mask-patterning techniques. In particular, the CDF requires spatially-coherent gratings spanning hundreds of microns, with precise control of pitch to $\sim 10^{-5}$ and appropriately placed phase steps of $(\pi/2) \pm 10^{-4}$ radians. As described in section 4.4, we are developing a spatial-phase-locked electron-beam lithography technique to achieve the required spatial fidelity in the x-ray masks.

4.16 Novel Superconducting Tunneling Structures

Sponsor

Defense Advanced Research Projects Agency
Consortium for Superconducting Electronics

Project Staff

Dr. Jack Chu,[7], Professor John M. Graybeal, Dr. Bernard S. Meyerson,[7] George E. Rittenhouse, Professor Henry I. Smith

In this project, we are studying the behavior of short-channel hybrid superconductor-degenerate semiconductor-superconductor (SSmS) Josephson devices, whose geometry is designed to display quantum electronic interference behavior. These studies include both theoretical and experimental examinations. This work represents the first examination of quantum interference effects for Cooper pairs via tunneling through extended resonant states. The characteristic energy scale for such a device would be set by the quantum confinement, and consequently may provide a new avenue for obtaining finite gains in Josephson three-terminal devices.

By numerically solving the Bogoliubov-deGennes equations for an SSmS junction, we have theoretically shown that the interference of ballistic

[7] IBM Corporation Cambridge, Massachusetts.

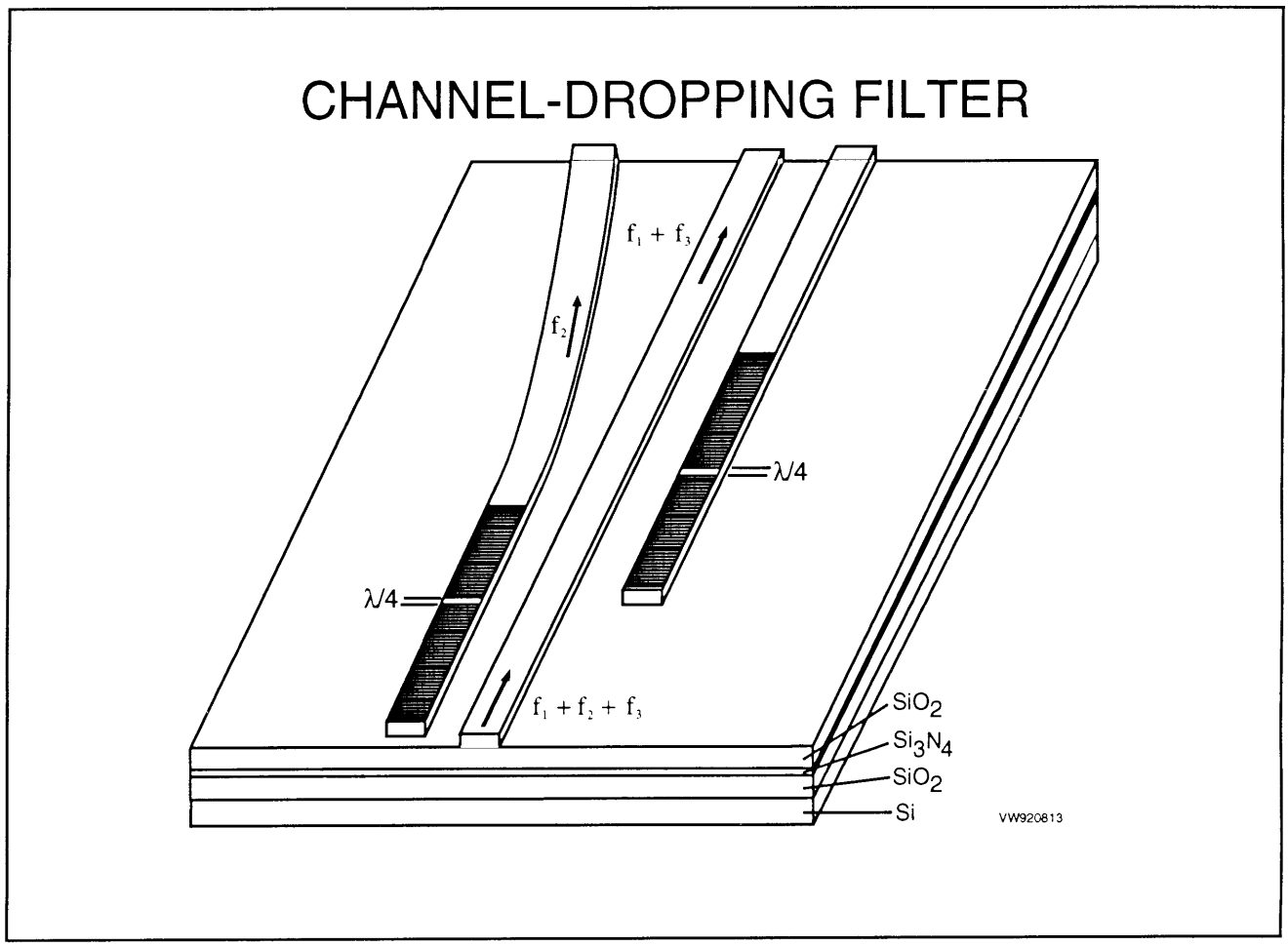

Figure 23. Structures of channel-dropping filter experiments on $SiO_2/Si_3N_4/SiO_2$.

Cooper pairs through spatially extended resonant states is indeed possible. As a function of the Fermi energy in the degenerate semi-conductor (i.e., as a function of electrostatic gate bias), we obtain striking cusp-shaped resonances in the Josephson critical current corresponding to the Fabry-Perot interference criteria. We find that such interference results regardless of how weakly coupled the quasi-bound states within the semiconductor layer are to the superconducting contacts. The coupling strength determines only the width and height of the cusp. Our calculations were performed assuming a one-dimensional system with a high-mobility semiconductor electron gas. The origin and nature of these resonances have been carefully analyzed, and differ markedly from those found in conventional non-superconducting resonant tunneling structures.

Note that our numerical solution to the Bogoliubov-deGennes equations can treat an arbitrary potential function within the semiconductor. We can thus consider a wide range of interesting and important junction geometries including conduction band mismatches, insulating interface or Schottky barriers, and intentionally introduced potentials within the N-layer which can enhance the quantum interferences. A key advantage of our technique is that it yields the full quasiparticle excitation spectrum within the Sm-layer as a function of the phase difference across the junction, thus providing important insight into the resultant physics.

We are exploring the fabrication of such a resonant tunneling Josephson junction using a high-mobility $Si:Si_{1-x}Ge_x$ two-dimensional electron gas (2DEG). A crucial and very demanding requirement of such a resonant SSmS structure is that the superconductor-semiconductor interface be clean and comparatively defect-free. The preferred electronic transport channel through the S-Sm interfaces is direct tunneling, as inelastic processes and/or tunneling through atomic localized states can be highly disruptive to the Cooper pair coherence. Presently, we are exploring superconductor-2DEG contacts using an intermediate phosphorous-implanted Si region. Optimizations of this contact

scheme are underway to improve their transmission of Cooper pairs.

4.17 Submicrometer-Period Transmission Gratings for X-ray and Atom-Beam Spectroscopy and Interferometry

Sponsor

Joint Services Electronics Program
Contract DAAL03-92-C-0001

Project Staff

James M. Carter, Julie C. Lew, Dr. Mark L. Schattenburg, Professor Henry I. Smith

Transmission gratings with periods of 100-1000 nm are finding increasing utility in applications such as x-ray, vacuum-ultraviolet, and atom-beam spectroscopy and interferometry. Over 20 laboratories around the world depend on MIT-supplied gratings in their work. For x-ray and VUV spectroscopy, gratings are made of gold and have periods of 100-1000 nm and thicknesses ranging from 100-1000 nm. They are most commonly used for spectroscopy of the x-ray emission from high-temperature plasmas. Transmission gratings are supported on thin (1 μm) polyimide membranes or made self supporting ("free standing") by the addition of crossing struts (mesh). (For short x-ray wavelengths membrane support is desired, while for the long wavelengths a mesh support is preferred in order to increase efficiency.) Fabrication is performed by holographic lithography, x-ray lithography and electroplating. Progress in this area focuses on improving the yield and flexibility of the fabrication procedures.

Another application is the diffraction of neutral sodium beams (de Broglie-wavelength ~ 17 pm) by mesh-supported gratings. Professor David Pritchard's group at MIT has clearly demonstrated atomic diffraction and interference. Because good spatial coherence (low distortion) of the grating is critical to ensure measurable interference of the beams, efforts are concentrated on the use of holographic lithography and the reactive-ion etching of free-standing gratings in low stress and high stiffness materials such as silicon nitride. This process is continuously being improved via an undergraduate thesis project. We also will use holographic interferometry (figure 5, section 4.3) to directly measure the spatial-phase fidelity of the free-standing nitride gratings.

4.18 High-Dispersion, High-Efficiency Transmission Gratings for Astrophysical X-ray Spectroscopy

Sponsor

National Aeronautics and Space Administration
Contract NAS8-36748

Project Staff

Professor Claude R. Canizares, Robert C. Fleming, Jr., Dr. Mark L. Schattenburg, Professor Henry I. Smith

This work involves a collaboration between the Center for Space Research and the Submicron Structures Laboratory (SSL), providing transmission gratings for the Advanced X-ray Astrophysics Facility (AXAF) x-ray telescope, currently scheduled for launch in 1998. Many hundreds of low-distortion, large-area transmission gratings of 200 nm period (gold) and 460 nm period (silver) are required. These will provide high resolution x-ray spectroscopy of astrophysical sources in the 100 eV to 10 keV band.

Because of the requirements of low distortion, high yield, and manufacturability, a fabrication procedure involving the replication of x-ray masks has been selected. Masks are made of high-stiffness silicon nitride membranes to eliminate distortion and patterned using a process involving holographic lithography, reactive-ion etching, and electroplating. The masks are then replicated using soft x-rays (1 - 1.5 nm) and the resulting patterns electroplated with gold or silver. An etching step then yields membrane-supported gratings suitable for space use. Flight prototype gratings have been fabricated and continue to undergo space-worthiness tests. Progress in this area focuses on increasing the yield and flexibility of the fabrication procedures, and the perfection of various mask and grating evaluation tests.

4.19 Submicron-Thickness X-ray Window Technology

Sponsor

National Aeronautics and Space Administration
Grant NAGW-2003
Contract NAS8-36748

Project Staff

Richard J. Aucoin, Nitin Gupta, Dr. Mark L. Schattenburg, Professor Henry I. Smith

We have been investigating various schemes for fabricating leak-free, large-area, ultrathin membranes to serve as vacuum isolation windows for the transmission of x-rays. Applications include gas-filled x-ray detector windows and high-vacuum isolation windows for x-ray lithography. Current window technology uses relatively thick beryllium windows which are opaque to x rays with wavelengths in the 0.5 - 1.5 nm band. However, this band is very useful for x-ray detector and x-ray lithography applications. Current efforts seek to perfect large-area polyimide windows which have a 1.0 micron thickness. When combined with tungsten or nickel meshes, these have been made leak free to the limit of He leak detector technology. Woven tungsten support meshes are used, and also advanced nickel meshes made by deep-etch x-ray lithography (so-called LIGA process), in collaboration with the MicroParts company in Germany. Future efforts will seek to reduce the membrane thickness still further, and also experiment with silicon nitride membranes which promise to be leak free and also bakeable for high vacuum applications. A silicon nitride isolation window is being used as a vacuum isolation window in our laboratory x-ray aligner. New high-strength nitrides, which we have developed using our dedicated in-house LPCVD system, promise to further improve window transmission.

4.20 GaAs Epitaxy on Sawtooth-Patterned Silicon

Sponsor

Joint Services Electronics Program
Contract DAAL 03-92-C-0001

Project Staff

Dr. Khalid Ismail, Nasser Karam,[8] Professor Henry I. Smith, Kenneth Yee

The growth of GaAs on Si offers the possibility of combining high-speed and optoelectronic GaAs devices with Si integrated-circuit technology. Oriented gratings of 200 nm period are fabricated in Si_3N_4 on (100) Si substrates. Anistrotropic etching in KOH is then used to produce sawtooth-profile gratings in the Si. Then these serve as substrates for GaAs growth by MOCVD. The dislocation density in the grown GaAs films is orders of magnitude lower than the density in films formed on planar Si substrates.

4.21 Publications

Journal Articles

Bagwell, P.F., S.L. Park, A. Yen, D.A. Antoniadis, H.I. Smith, T.P. Orlando, and M.A. Kastner. "Magnetotransport in Multiple Narrow Silicon Inversion Channels Opened Electrostatically into a Two-Dimensional Electron Gas." *Phys. Rev.* B 45: 9214-9221 (1992).

Carter, J.M., D.B. Olster, M.L. Schattenburg, A. Yen, and H.I. Smith. "Large-Area, Free-Standing Gratings for Atom Interferometry Produced Using Holographic Lithography." *J. Vac. Sci. Technol. B* 10: 2909-2911 (1992).

Chu, W., H.I. Smith, S.A. Rishton, D.P. Kern, and M.L. Schattenburg. "Fabrication of 50 nm Line-and-Space X-ray Masks in Thick Au using a 50 keV Electron Beam System." *J. Vac. Sci. Technol. B* 10: 118-121 (1992).

Chu, W., C.C. Eugster, A. Moel, E.E. Moon, J.A. del Alamo, H.I. Smith, M.L. Schattenburg, K.W. Rhee, M.C. Peckerar, and M.R. Melloch. "Conductance Quantization in a GaAs Electron Waveguide Device Fabricated by X-ray Lithography." *J. Vac. Sci. Technol. B* 10: 2966-2969 (1992).

Ghanbari, R.A., M. Burkhardt, D.A. Antoniadis, H.I. Smith, M.R. Melloch, K.W. Rhee, and M.C. Peckerar. "Comparative Mobility Degradation in Modulation-Doped GaAs Devices after E-beam and X-ray Irradiation." *J. Vac. Sci. Technol. B* 10: 2890-2892 (1992).

Ghanbari, R.A., W. Chu, E.E. Moon, M. Burkhardt, K. Yee, D.A. Antoniadis, H.I. Smith, M.L. Schattenburg, K.W. Rhee, R. Bass, M.C. Peckerar, and M.R. Melloch. "Fabrication of Parallel Quasi-One-Dimensional Wires Using a Novel Conformable X-ray Mask Technology." *J. Vac. Sci. Technol. B* 10: 3196-3199 (1992).

Hector, S.D., M.L. Schattenburg, E.H. Anderson, W. Chu, V.V. Wong, and H.I. Smith. "Modeling and

[8] Spire Corporation.

Experimental Verification of Illumination and Diffraction Effects on Image Quality in X-ray Lithography." *J. Vac. Sci. Technol. B* 10: 3164-3168 (1992).

Ku, Y.C., M.H. Lim, J.M. Carter, M.K. Mondol, A. Moel, and H.I. Smith. "Correlation of In-Plane and Out-of-Plane Distortion in X-ray Lithography Masks." *J. Vac. Sci. Technol. B* 10: 3169-3172 (1992).

Rhee, K.W., D.I. Ma, M.E. Peckerar, R.A. Ghanbari, and H.I. Smith. "Proximity Effect Reduction in X-ray Mask Making Using Thin Silicon Dioxide Layers." *J. Vac. Sci. Technol. B* 10: 3062-3066 (1992).

Rittenhouse, G.E., K. Early, B.S. Meyerson, H.I. Smith, and J.M. Graybeal. "Novel Vertical Silicon-Membrane Structure and Its Application to Josephson Devices." *J. Vac. Sci. Technol. B* 10: 2860-2863 (1992).

Smith, H.I., and M.L. Schattenburg. "X-ray Lithography, from 500 to 30 nm: X-ray Nanolithography." Submitted to *IBM J. Res. Dev.* as part of a special issue on X-ray Lithography (1993).

Yen, A., M.L Schattenburg, and H.I. Smith. "A Proposed Method for Fabricating 50 nm-period Gratings by Achromatic Holographic Lithography." *Appl. Opt.* 31: 2972-2973 (1992).

Yen, A., E.H. Anderson, R.A. Ghanbari, M.L. Schattenburg, and H.I. Smith. "Achromatic Holographic Configuration for 100 nm Period Lithography." *Appl. Opt.* 31: 4540-4545(1992).

Yen, A., H.I. Smith, M.L. Schattenburg, and G.N. Taylor. "An Anti-Reflection Coating for use with PMMA at 193 nm." *J. Electrochem. Soc.* 139: 616-619 (1992).

Zhao, Y., D.C. Tsui, M. Santos, M. Shayegan, R.A. Ghanbari, D.A. Antoniadis, and H.I. Smith. "Magneto-optical Absorption in a Two Dimensional Electron Grid." *Appl. Phys. Lett.* 12: 1510-1512 (1992).

Meeting Papers

Canizares, C.R., D. Dewey, E.B. Galton, T.H. Markert, H.I. Smith, M.L. Schattenburg, B.E. Woodgate, and S. Jordan. "The MIT High Resolution X-ray Spectroscopy Instruments on AXAF." Paper presented at AIAA Space Programs and Technologies Conference, Huntsville, Alabama, March 24-27, 1992.

Kumar, A. "Electron States and Potentials in Quantum Dot Structures." Paper presented at the American Physical Society Symposium on Charging Effects in Quantum Dots, Indianapolis, Indiana. *Bull. Amer. Phys. Soc.* 37: 429 (1992).

Smith, H.I., and D.A. Antoniadis. "Mesoscopic Devices: Will They Supersede Transistors in ULSI?" Paper presented at the International Conference on Solid State Devices and Materials, Tsukuba, Japan, August 26-28, 1992.

Smith, H.I. "History of X-ray Lithography." Paper presented at Optcon '92, Boston, Massachusetts, November 15-20, 1992.

Smith, H.I., and M.L. Schattenburg. "Proximity X-ray Nanolithography P Current Performance and Theoretical Limits." Paper presented at the 39th National Symposium American Vacuum Society, Chicago, Illinois, November 9-12, 1992.

Smith, H.I., and M.L. Schattenburg. "Why Bother with X-ray Lithography?" Proceedings of the SPIE Symposium Microlithography, San Jose, California, March 8-13, 1992.

Zhao, Y., D.C. Tsui, K. Hirakawa, M. Santos, M. Shayegan, R.A. Ghanbari, D.A. Antoniadis, and H.I. Smith. "Far Infrared Magneto-Absorption by the 2DEG in GaAs/AlGaAs Heterostructures with Grid Gates." Paper presented at the 21st International Conference on the Physics of Semiconductors, Bejing, China, August 10-14, 1992.

Zhao, Y., D.C. Tsui, K. Hirakawa, M. Santos, M. Shayegan, R. Ghanbari, D.A. Antoniadis, and H.I. Smith. "Far Infrared Magneto-Absorption by the 2 DEG in GaAs/AlGaAs Heterostructures with Grid Gates." Paper presented at the American Physical Society Meeting, Indianaopoilis, Indiana, March 16-20, 1992.

Theses

Modiano, A.M. *An Aligner for X-ray Nanolithography.* Ph.D. diss. Dept. of Electr. Eng. and Comput. Sci., MIT, May 1992.

Olster, D.B. *Refining the Process of Achromatic Holographic Lithography.* S.B. thesis, Dept. of Electr. Eng. and Comput. Sci., MIT, May 1992.

MIT Patents

Smith, H.I., E.H. Anderson, and M.L. Schattenburg. "Holographic Lithography." Patent 5,142,385, August 25, 1992.

Smith, H.I., E.H. Anderson, and M.L. Schattenburg. "Energy Beam Locating." Patent 5,136,169, August 4, 1992.

Books/Chapters in Books

Bagwell, P.F., A. Kumar, and R. Lake. "Scattering and Quantum Localization of Electrons in a Waveguide by Static and Time-Varying Potentials." In *Quantum Effect Physics, Electronics and Applications.* Eds. Ismail, T. Ikoma, and H.I. Smith. Philadelphia: Institute of Physics Publishing, 1992, chapter 2, p. 45.

Ismail, K., T. Ikoma, and H.I. Smith, *Quantum Effect Physics, Electronics and Applications.* Institute of Physics Conference Series Number 127, Philadelphia: Institute of Physics Publishing, 1992.

Smith, H.I., and M.L. Schattenburg. "Lithography for Manufacturing at 0.25 Micrometer and Below." In *Crucial Issues in Semiconductor Materials and Processing Technologies.* NATO ASI Series E, 222: 153. Eds. S. Coffa, F. Priolo, E. Rimini, and J.M. Poate. 1992.